Pressure derivatives of the elastic moduli of the rutile-structure difluorides

D. Gerlich,* S. Hart, and D. Whittal
National Institute for Materials Research, Council for Scientific and Industrial Research, P.O. Box 395, Pretoria 0001, South Africa
(Received 26 August 1983)

The pressure derivatives of the elastic moduli of single-crystal CoF_2 and MnF_2 have been determined from the variation of the sound velocity under hydrostatic pressure. All pressure derivatives of the rutile-structure difluorides decrease slightly with increasing cation radius. From the pressure derivatives, the elastic-mode Grüneisen γ's and the low- and high-temperature limits of the Grüneisen constant are derived and compared with the thermodynamic values, a fair agreement being found for the high-temperature values. The experimental values of the pressure derivatives are compared with theoretical values derived from a rigid-ion central-force-interaction model and the agreement is found to improve with increasing cation radius.

I. INTRODUCTION

The rutile-structure difluorides, RF_2 (R=Mg, Ni, Co, Zn, Fe, or Mn), constitute an interesting series of materials because of their geophysical importance on the one hand, and also due to the series of phase transitions that they undergo under the influence of pressure and temperature.[1-3] The compounds are structurally related to stishovite, which presumably plays a vital role in the structure of the lower mantle of the earth. Also, all of them undergo a series of structural phase transformations from rutile to distorted fluorite and finally to a post-distorted fluorite form ($PbCl_2$ or hexagonal). Hence, many varied investigations of these substances have been undertaken in the past.

In this paper measurements of the pressure dependence of the elastic moduli on single crystals of CoF_2 and MnF_2 are described. This investigation may provide additional information on the relation between the lattice dynamics of these materials, especially the softening slow shear mode associated with the shear constant $c_s=\frac{1}{2}(c_{11}-c_{12})$ and its relation to the phase transformation. Also, the modified Born criterion[4] and its connection with the phase transition may be examined. The various mode-Grüneisen γ's and the low- and high-temperature limits of the Grüneisen constant will be evaluated from the elastic data and compared to the corresponding thermodynamic values whenever the latter are available.

II. EXPERIMENTAL

Single crystals of CoF_2 and MnF_2 were grown by the Stockbarger method in a vacuum furnace. The starting powder material was loaded into graphite crucibles with a 90° cone angle, and the required temperature distribution was obtained from a profiled graphite heating element supplied by the mains frequency at low voltage and high current. When suitably baffled using molybdenum radiation screens, a temperature gradient of about 50 $K\,cm^{-1}$ was obtained. Growth speeds were of the order of 1.5 $mm\,h^{-1}$. MnF_2 was grown under vacuum, while CoF_2 was grown under a positive pressure of 200 mbar of oxygen-free nitrogen. Typical impurity levels in MnF_2 were 100 ppm of Mg, while for CoF_2 they were 100 ppm of Fe, 70 ppm of Ni, 10 ppm of Mg, and 10 ppm of Mn.

The specimens were oriented by means of x-ray Laue back reflection photographs. On each sample a number of pairs of flat and parallel faces corresponding to crystalline planes of high symmetry were cut and lapped. The pressure derivatives were determined by measuring the change in the velocity of ultrasonic longitudinal and shear waves, 10 MHz frequency, propagating along various crystalline directions of high symmetry under hydrostatic pressure in the range 0—1 GPa. The sound waves were generated by crystalline-quartz transducers bonded to one face by a 1:1 formula weight mixture of glycerine and phthalic anhydride, while the velocity was determined by the pulse-echo—overlap method. The pressure was generated in a piston-cylinder apparatus utilizing a 1:1 mixture by volume of n-pentane and isopentane as the pressurizing medium. A detailed description of the ultrasonic and high-pressure techniques has been published elsewhere.[5]

III. RESULTS

In Table I the various physical parameters of the rutile-structure difluorides required for the subsequent data evaluation are presented.[6-9] Here a and c are the lattice parameters of the tetragonal unit cell, u is the parameter defining the nearest-neighbor anion-cation distance in the cell as $\sqrt{2}au$, R_+ is the Pauling cation radius,[9] ρ is the density, c_{ij} and s_{ij} are the six independent adiabatic elastic stiffness and compliance moduli, κ_v^s and κ_v^T are the adiabatic and isothermal compressibilities, B^T is the isothermal bulk modulus, α_a and α_c denote, respectively, the linear thermal expansion in the a and c directions, and C_p is the specific heat at constant pressure. All values refer to room temperature. As can be seen, the difference between the isothermal and adiabatic elastic moduli is negligible and no differentiation between the two sets will be made.

Figures 1—4 show the experimental values of the natural modulus, defined as $\rho_0 W^2$, where ρ_0 is the zero-pressure density, and W is the natural velocity[10] as a function of the pressure P for a number of propagation directions and modes. The solid circles in these figures are the experi-

TABLE I. Various physical parameters for the rutile-structure difluorides.

	MgF_2	NiF_2	CoF_2	ZnF_2	MnF_2
a (Å)	4.623	4.651	4.695	4.703	4.873
c (Å)	3.052	3.048	3.180	3.134	3.310
u	0.303	0.302	0.306	0.303	0.305
R_+ (Å)	0.65	0.70	0.72	0.74	0.80
ρ (kg/m^3)	3177	4815	4592	4952	3922
c_{11} (GPa)	140.6	145.0	128.1	130.0	103.3
c_{12} (GPa)	90.2	110.0	100.0	96.7	82.7
c_{13} (GPa)	62.9	90.9	88.1	89.0	70.2
c_{33} (GPa)	205.1	220.8	197.1	199.2	166.0
c_{44} (GPa)	56.6	46.5	37.6	39.5	31.7
c_{66} (GPa)	95.8	99.4	85.5	81.4	70.0
s_{11} (10^{-11} Pa^{-1})	1.25	1.71	2.11	1.82	2.82
s_{12} (10^{-11} Pa^{-1})	−0.73	−1.15	−1.44	−1.14	−2.03
s_{13} (10^{-11} Pa^{-1})	−0.16	−0.23	−0.30	−0.30	−0.33
s_{33} (10^{-11} Pa^{-1})	0.59	0.64	0.77	0.78	0.88
s_{44} (10^{-11} Pa^{-1})	1.77	2.15	2.66	2.56	3.15
s_{66} (10^{-11} Pa^{-1})	1.04	1.01	1.17	1.24	1.43
κ_v^S (10^{-11} Pa^{-1})	0.99	0.84	0.91	0.95	1.14
κ_v^T (10^{-11} Pa^{-1})	1.00	0.84	0.92	0.96	1.15
B^T (GPa)	100.1	119.0	108.7	103.8	88.1
α_a (10^{-6} K^{-1})	9.4	7.19	3.67	8.97	3.63
α_c (10^{-6} K^{-1})	13.60	9.04	10.33	11.64	12.87
C_p (J/kg)	988.4	662.4	709.6	635.1	569.5

mentally measured data points, while the straight lines are linear least-squares fits to the experimental data. From the slopes of these lines the pressure derivative of ρv^2 for $P=0$, $(\rho v^2)'_0$, where ρ and v are, respectively, the density and velocity at pressure P, may now be determined. For a particular propagation direction and mode, the connection between $(\rho v^2)'_0$ and the values of the natural modulus and its pressure derivative at $P=0$, i.e., $(\rho_0 W^2)'_0$, is given by

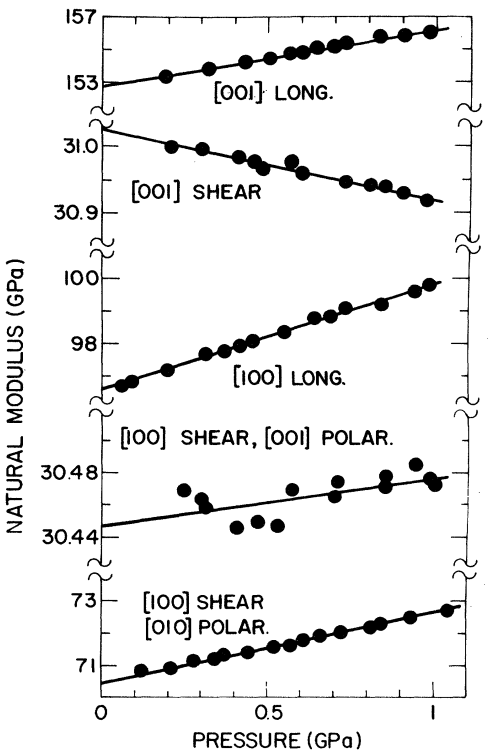

FIG. 1. Natural modulus as a function of pressure for various propagation directions and modes in CoF_2.

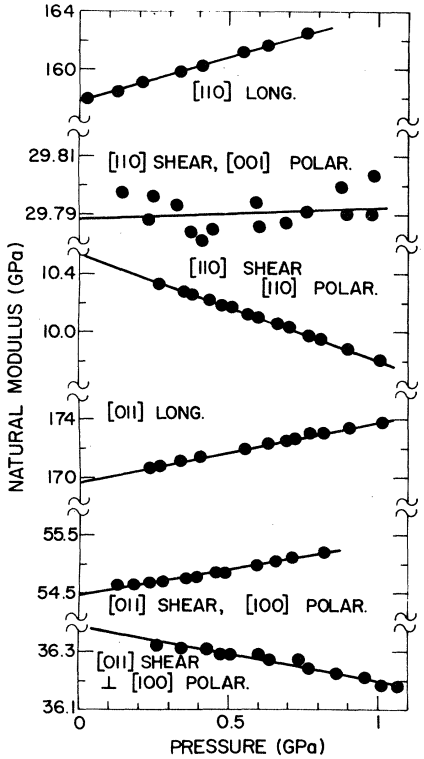

FIG. 2. Natural modulus as a function of pressure for various propagation directions and modes in CoF_2.

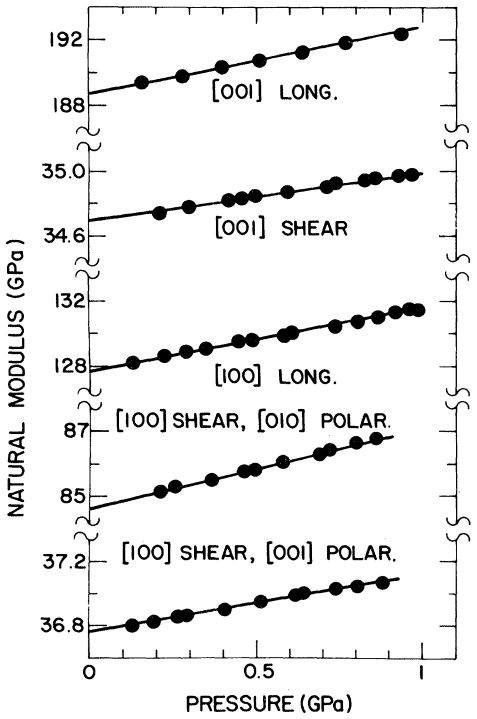

FIG. 3. Natural modulus as a function of pressure for various propagation directions and modes in MnF_2.

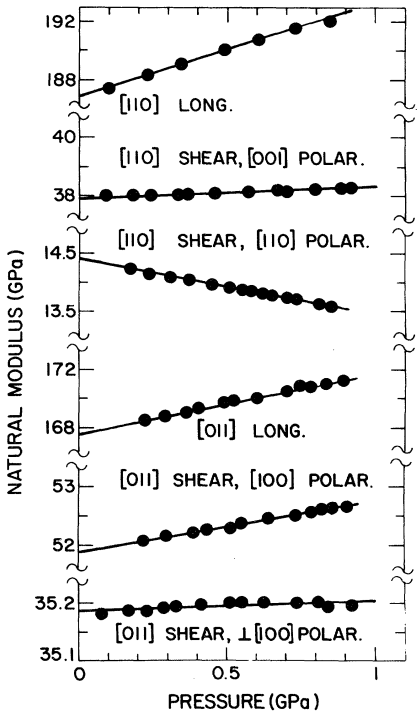

FIG. 4. Natural modulus as a function of pressure for various propagation directions and modes in MnF_2.

$$(\rho v^2)'_0=(\rho_0 W^2)'_0+(\rho_0 W^2)_0(\kappa_v-2\kappa_l)\ , \tag{1}$$

where κ_l is the linear compressibility for the particular propagation direction. If $\vec{N}$ is the unit vector in the propagation direction, κ_l will be given by

$$\kappa_l=(s_{11}+s_{12}+s_{13})(N_1^2+N_2^2)+(2s_{13}+s_{33})N_3^2\ . \tag{2}$$

In Table II the relation between $(\rho v^2)'$ and $(\rho_0 W^2)'_0$ for the various propagation directions and modes is shown. In the propagation direction and mode column, the first direction designates the propagation, and the second direction designates the polarization. In Table III the experimental values for $(\rho_0 W^2)'_0$, together with their associated

TABLE II. Relation between $(\rho v^2)'_0$ for various propagation directions and modes.

Propagation direction and mode	$(\rho v^2)_0$	$(\rho v^2)'_0$
[001], [001]	c_{33}	$(\rho_0 W^2)'_0+c_{33}(2s_{11}+2s_{12}-s_{33})$
[001], [001]	c_{44}	$(\rho_0 W^2)'_0+c_{44}(2s_{11}+2s_{12}-s_{33})$
[100], [100]	c_{11}	$(\rho_0 W^2)'_0+c_{11}(2s_{13}+s_{33})$
[100], [001]	c_{44}	$(\rho_0 W^2)'_0+c_{44}(2s_{13}+s_{33})$
[100], [010]	c_{66}	$(\rho_0 W^2)'_0+c_{66}(2s_{13}+s_{33})$
[100], [110]	c_L	$(\rho_0 W^2)'_0+c_L(2s_{13}+s_{33})$
[110], [1$\bar{1}$0]	c_s	$(\rho_0 W^2)'_0+c_s(2s_{13}+s_{33})$
[110], [001]	c_{44}	$(\rho_0 W^2)'_0+c_{44}(2s_{13}+s_{33})$
[011], [011]	c_{QL}	$(\rho_0 W^2)'_0+c_{QL}(\kappa_v-2\kappa_{011})$
[011], [100]	c_T	$(\rho_0 W^2)'_0+c_T(\kappa_v-2\kappa_{011})$
[011], ⊥[100]	c_{QT}	$(\rho_0 W^2)'_0+c_{QT}(\kappa_v-2\kappa_{011})$

$$c_L=\tfrac{1}{2}(c_{11}+c_{12}+2c_{66}),\quad c_s=\tfrac{1}{2}(c_{11}-c_{12}),\quad c_T=m^2c_{66}+n^2c_{44}{}^{a}$$

$$c_{QL}=\tfrac{1}{2}((c_{11}m^2+c_{33}n^2+c_{44})+\{[c_{11}m^2-c_{33}n^2+c_{44}(n^2-m^2)]^2+4m^2n^2(c_{13}+c_{44})^2\}^{1/2})^{a}$$

$$c_{QT}=\tfrac{1}{2}((c_{11}m^2+c_{33}n^2+c_{44})-\{[c_{11}m^2-c_{33}n^2+c_{44}(n^2-m^2)]+4m^2n^2(c_{13}+c_{44})^2\}^{1/2})^{a}$$

$$\kappa_v=2s_{11}+s_{33}+2(s_{12}+2s_{13}),\quad \kappa_{011}=(s_{11}+s_{12}+s_{13})m^2+(2s_{13}+s_{33})n^{2a}$$

[a] m and n are the direction cosines of the [011] direction with respect to the [010] and [001] axes.

TABLE III. Values of $(\rho_0 W^2)'_0$ and $(\rho v^2)'_0$ for the various propagation directions and modes in CoF_2 and MnF_2.

Propagation mode and directon	CoF_2 $(\rho_0 W^2)'_0$	CoF_2 $(\rho v^2)'_0$	MnF_2 $(\rho_0 W^2)'_0$	MnF_2 $(\rho v^2)'_0$
[001], [001]	3.99 ±0.07	5.11	3.45 ±0.05	4.61
[001], [001]	0.300±0.008	0.51	−0.110±0.005	0.11
[100], [100]	3.81 ±0.06	4.03	3.23 ±0.1	3.46
[100], [001]	0.351±0.003	0.41	0.03 ±0.01	0.10
[100], [010]	2.46 ±0.02	2.61	2.17 ±0.02	2.32
[110], [110]	6.38 ±0.11	6.72	6.08 ±0.05	6.44
[110], [1$\bar{1}$0]	−0.948±0.005	−0.93	−0.710±0.003	−0.69
[110], [001]	0.373±0.009	0.43	0.004±0.006	0.07
[011], [011]	4.06 ±0.06	4.86	4.03 ±0.04	4.82
[011], [100]	0.877±0.007	1.12	0.90 ±0.03	1.14
[011], ⊥[100]	0.017±0.005	0.18	−0.18 ±0.01	−0.02

errors and the corresponding values of $(\rho v^2)'_0$ derived from the latter, are presented. From these values of $(\rho v^2)'_0$, the pressure derivatives of elastic moduli $\partial c_{ij}/\partial P$ may now be determined. As there are 11 equations for the six unknowns, the system is overdetermined and the values of the $\partial c_{ij}/\partial P$ were computed by a least-squares fit, the results being shown in Table IV together with Manghnani's data[11] for MnF_2. As can be seen, the agreement between the two latter sets is generally satisfactory except in the case of $\partial c_{13}/\partial P$ and $\partial c_{66}/\partial P$.

IV. DISCUSSION

A. Correlation with cation radius

The rutile-structure diflourides form an isomorphous series with the same anion where the cation radius increases monotonically from Mg^{2+} to Mn^{2+}. In Fig. 5 the correlation between the pressure derivatives of the various elastic moduli and the Pauling cation radius[9] is examined. As can be seen, the pressure derivatives generally decrease slightly with increasing cation radius, a phenomenon which is also manifested by the elastic moduli themselves.[6]

B. Grüneisen-mode γ's

Assuming an anisotropic continuum and Debye model, the mode-Grüneisen γ's γ_i, may be related directly to the elastic moduli and their pressure derivatives.[12] For a particular propagation mode i one obtains

$$\gamma_i = \frac{B}{2(\rho v_i^2)_0}(\rho v_i^2)'_0 + B\kappa_l - \tfrac{1}{2} . \tag{3}$$

If $N(i)$ and $U(i)$ are unit vectors in the propagation and polarization directions, then

$$(\rho v_i^2)'_0 = \frac{\partial c_{klmn}}{\partial P} N_k(i) N_m(i) U_l(i) U_n(i) , \tag{4}$$

with the subscripts k, l, m, and n denoting Cartesian components, summation over repeated indices being assumed, and c_{klmn} denoting the fourth-rank tensor components of

TABLE IV. Pressure derivatives of the elastic moduli of CoF_2 and MnF_2.

	CoF_2	MnF_2	MnF_2 (Manghnani *et al.*)[a]
$\partial c_{11}/\partial P$	4.58	3.50	3.56
$\partial c_{12}/\partial P$	5.46	4.72	5.08
$\partial c_{13}/\partial P$	4.37	4.62	3.87
$\partial c_{33}/\partial P$	4.98	4.74	4.95
$\partial c_{44}/\partial P$	0.42	0.22	0.14
$\partial c_{66}/\partial P$	4.81	2.98	4.16
$\partial B/\partial P$	4.81	4.29	4.21

[a]Reference 11.

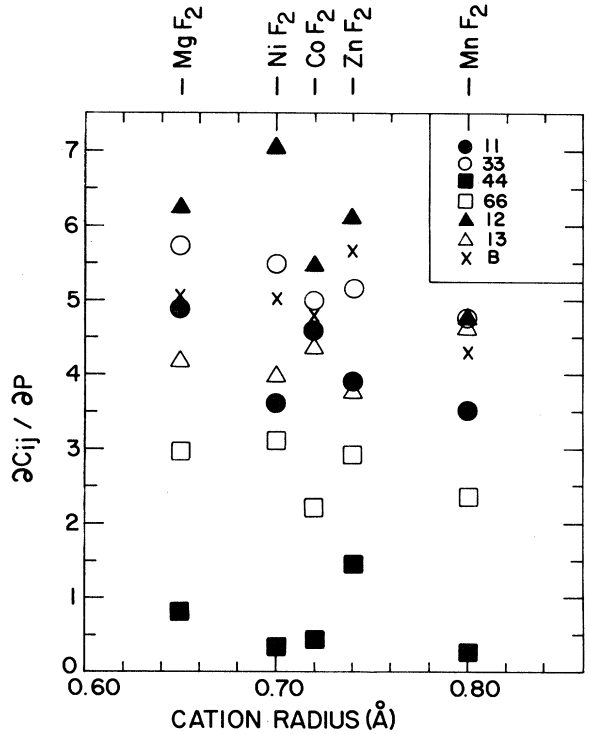

FIG. 5. Pressure derivatives of the elastic moduli as a function of the cation radius.

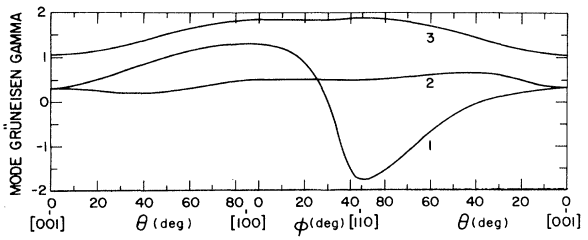

FIG. 6. Mode-Grüneisen γ parameters in some crystalline directions of high symmetry for CoF_2.

the elastic stiffness moduli. From the mode γ's, the low- and high-temperature limits of the elastic Grüneisen constant, γ_0^{el} and γ_H^{el}, may now be evaluated as follows:

$$\gamma_0^{el}=\frac{\sum_i(\rho v_i^2)_0^{-3/2}\gamma_i}{\sum_i(\rho v_i^2)_0^{-3/2}}\,, \tag{5}$$

$$\gamma_H^{el}=\frac{1}{Q}\sum_i\gamma_i\,, \tag{6}$$

Q being the number of modes summed.

Utilizing Eqs. (3) and (4), the mode γ's for some directions of high symmetry were calculated and the results are shown in Figs. 6 and 7. Here 1 and 2 designate the slow and fast shear modes, and 3 denotes the longitudinal mode. It is evident that in the case of MnF_2 the mode γ's for the slow shear mode are essentially negative over the whole range, which may indicate, at low temperatures where the slow shear mode is the one mainly excited, that the thermal expansion may become negative. This is borne out by Table V where γ_0^{el} and γ_H^{el} are compared with the corresponding values of the thermodynamic Grüneisen constant γ^{th} determined from the thermal expansion and specific heat. As can be seen, γ^{th} at 80 K is negative, indicating a negative thermal expansion at low temperatures.

C. Comparison with theoretical values

Based on a rigid-ion model with a central-force short-range interaction between nearest-neighbor cation-anions and anion-anions, in addition to the usual Coulomb interaction, Striefler and Barsch[13,14] have calculated the pressure derivatives of the elastic moduli for the rutile-structure difluorides. Their theoretical values together with the experimental data are shown in Table VI. Also included in the same table is a quality of agreement parameter between the two sets of experimental and theoretical values for the six independent pressure derivatives $\partial c_{ij}/\partial P$. This parameter is defined as the square root of the sum of the squares of the deviations divided by 6×5. As can be seen, the agreement between experiment and theory is generally appreciably better for the substances with the larger cation radius than for MgF_2 with the smallest cation radius.

TABLE V. Comparison of the low- and high-temperature limits of the elastic Grüneisen constant with the thermodynamics Grüneisen constant.

	γ_0^{el}	γ^{th} (80 K)	γ_0^{el}	γ^{th} (300 K)
MgF_2	0.41		0.87	1.03
NiF_2	−0.59		0.53	0.87
CoF_2	0.22		0.81	0.59
ZnF_2	0.54		1.17	0.98
MnF_2	−0.24	−0.02	0.52	0.79

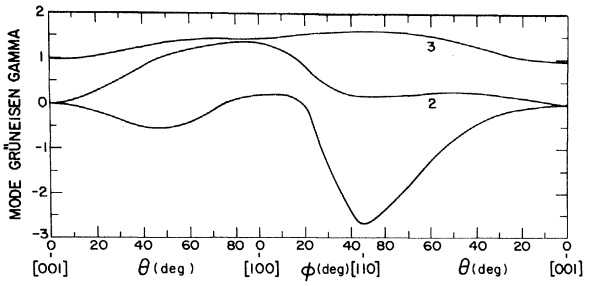

FIG. 7. Mode-Grüneisen γ parameters in some crystalline directions of high symmetry for MnF_2.

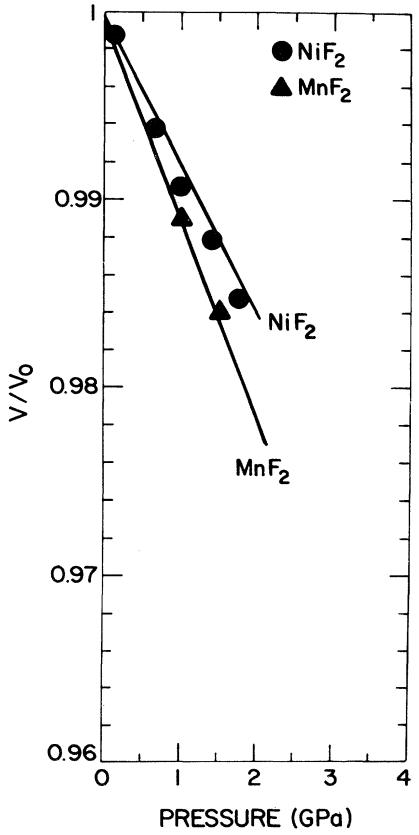

FIG. 8. Equation of state for NiF_2 and MnF_2.

TABLE VI. Comparison of experimental data and theoretical values for the pressure derivatives of the elastic moduli.

	$\partial c_{11}/\partial P$		$\partial c_{33}/\partial P$		$\partial c_{12}/\partial P$		$\partial c_{13}/\partial P$		$\partial c_{44}/\partial P$		$\partial c_{44}/\partial P$		Quality
	Expt.	Theor.	Expt.	Theor.	Expt.	Theor.	Expt.	Theor.	Expt.	Theor.	Expt.	Theor.	of fit
MgF_2	4.92	2.23	5.74	2.73	6.22	3.83	4.15	4.46	0.79	−1.29	2.97	1.85	1.1
NiF_2	3.60		5.48		7.04		4.45		0.29		3.10		
CoF_2	4.58	5.20	4.98	4.44	5.46	6.81	4.37	5.93	0.42	−1.42	2.18	4.46	0.6
ZnF_2	3.88	4.15	5.16	3.94	6.11	5.83	3.78	5.40	1.46	−1.42	2.89	3.50	0.6
MnF_2	3.50	2.17	4.74	3.06	4.72	4.13	4.62	4.54	0.22	−1.78	2.36	2.15	0.5

D. Equation of state in the low-pressure (rutile) phase

Utilizing the measured values of the bulk modulus and its pressure derivative B', an equation of state (pressure-volume relation) for the material may be constructed.[15] One which is widely used is the Murnaghan first-order equation of state,

$$\frac{V}{V_0}=\left[1+\frac{B'}{B}P\right]^{-1/B'}, \tag{7}$$

where V is the volume and V_0 is its zero-pressure value. In Fig. 8 the solid lines represent the above equation for NiF_2 and MnF_2, while the solid circles and solid triangles represent the experimental data.[16,17] As can be seen, the agreement between the Murnaghan equation and the experimental data is very good, which is really not surprising since the low-pressure phase extends only over a small pressure range in these materials.

ACKNOWLEDGMENTS

One of us (D.G.) wishes to thank the Council for Scientific and Industrial Research (South Africa) for the award of a visiting appointment during the tenure of which the present work was carried out.

*On sabbatical leave from the Department of Physics and Astronomy, Tel Aviv University, Ramat Aviv, Tel Aviv 69978, Israel.

[1]J. C. Jamieson, in *High Pressure Research,* edited by M. H. Manghnani and S.-I. Akimoto (Academic, New York, 1977), p. 209.

[2]L. C. Ming, M. H. Manghnani, T. Matsui, and J. C. Jamieson, Phys. Earth Planet. Inter. 23, 276 (1980).

[3]M. H. Manghnani, L. C. Ming, and T. Matsui, in *High Pressure Science and Technology,* edited by B. Vodar and Ph. Marteau (Pergamon, Oxford, 1980), p. 1092.

[4]H. H. Demarest, Jr., R. Ota, and O. L. Anderson, in *High Pressure Research,* Ref. 1, p. 281.

[5]S. Hart and P. H. Greenwood, Solid State Commun. 46, 161 (1983).

[6]S. Hart, S. Afr. J. Phys. 1, 65 (1978).

[7]R. S. Krishnan, R. Srinivasan, and S. Devanarayanan, *Thermal Expansion of Crystals* (Pergamon, Oxford, 1979).

[8]H. H. Landolt-Börnstein, *Zahlenwerte und Funktionen,* 6th ed. (Springer, Berlin, 1961) (in German), Vol. II, Part 4.

[9]L. Pauling, *The Nature of the Chemical Bond* (Cornell University Press, Ithaca, New York, 1967), p. 514.

[10]R. N. Thurston and K. Brugger, Phys. Rev. 133, A1604 (1964).

[11]M. H. Manghnani, T. Matsui, and J. C. Jamieson, Trans. Am. Geophys. Union EOS 60, 387 (1979).

[12]K. Brugger and T. C. Fritz, Phys. Rev. 157, 524 (1967).

[13]M. E. Striefler and G. R. Barsch, Phys. Status Solidi B 59, 205 (1973).

[14]M. E. Striefler and G. R. Barsch, Phys. Status Solidi B 64, 613 (1974).

[15]O. L. Anderson, J. Phys. Chem. Solids 27, 547 (1966).

[16]J. D. Jorgensen and T. G. Worlton, Phys. Rev. B 17, 2212 (1978).

[17]R. M. Hazen and L. W. Finger, J. Phys. Chem. Solids 42, 143 (1981).